Food Chemistry: X 21 (2024) 101117

Contents lists available at ScienceDirect

Food Chemistry: X

journal homepage: www.sciencedirect.com/journal/food-chemistry-x

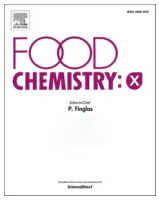

Improvement of oxidized myofibrillar protein gel properties by black rice extract

Huali Wang [a], Matthew Kay [b], Daojiu Zhang [c], Guijie Chen [d,*], Xiang Li [b,*]

[a] China National Center for Food Safety Risk Assessment, Beijing 100022, China
[b] School of Marine and Biological Engineering, Yancheng Teachers' University, Yancheng 224007, China
[c] Inner Mongolia Hulunbeir Arong Banner Agricultural Development Center, Hulunbeir Arong Banner, China
[d] State Key Laboratory of Tea Plant Biology and Utilization, School of Tea & Food Science and Technology, Anhui Agricultural University, Hefei 230036, China

ARTICLE INFO

Keywords:
Black rice extract
Myofibrillar protein
Oxidation
Physicochemical properties
Gel properties

ABSTRACT

In order to investigate the effects of black rice extract (BE) on the composition of oxidized myofibrillar protein (MP) gel, different concentrations of BE (0, 10, 20, 50 mg g^{-1}) were analyzed experimentally. Results revealed that the addition of small doses of BE significantly inhibited the formation of carbonyl groups in oxidized MP, and improved surface hydrophobicity and gel water holding capacity. Additionally, 10 and 20 mg g^{-1} BE increased the ordered structure of oxidized MP. Furthermore, dynamic rheometer results showed a significant increase in the storage modulus (G') of oxidized MP with 10 and 20 mg g^{-1} BE during heating. Scanning Electron Microscopy (SEM) showed that MP formed a denser network structure with addition of 10 and 20 mg g^{-1} BE. Low-Field Nuclear Magnetic Resonance (LF-NMR) and magnetic resonance imaging (MRI) showed that there is a significant increase in immobile water in MP gel and a decrease in free water within the 20 mg g^{-1} BE group. In conclusion, 20 mg g^{-1} supplemented BE significantly improved the structure order and hardness of oxidized MP gel, increased its structure density and water holding capacity, and it provides a theoretical basis for the application of antioxidants in meat products.

1. Introduction

Protein oxidation is an inevitable natural phenomenon in the industry of muscle food processing and long-term storage (Fuentes-Lemus & López-Alarcón, 2020). It can lead to protein crosslinking, sulfhydryl loss, the formation of carbonyl compounds and other changes in physical and chemical properties (Classics Lowry, Rosebrough, Farr, & Randall, 1951; Davies, 2016). The change of myofibrillar protein structure can further lead to the deterioration of protein function, such as water holding capacity, emulsification performance and meat tenderness, which will affect the quality and sales of meat and can even cause harm to human body. Antioxidants can remove reactive oxygen species (ROS) and prevent oxidation attacks on other substances (Cheng et al., 2019; Rosenfeld, Vasilyeva, Yurina, & Bychkova, 2018). Therefore, in recent years, adding antioxidants to meat or meat products has become an effective protective measure, especially with the use of plant extracts rich in phenols (Cheng, Xu, Xiang, Liu, & Zhu, 2020; Huang et al., 2022). It has been shown that polyphenols derived from fruits, vegetables, herbs and spices have a positive effect on inhibiting protein oxidation in meat and meat products (Guo & Xiong, 2021).

Phenolic compounds contain large numbers of hydroxyl groups, which can be oxidized to form quinone compounds. This intermediate can spontaneously interact with proteins in the form of covalent bonds, resulting in structural changes (Wang et al., 2020; Yan et al., 2020). For example, α-casein, β-casein, α-whey protein, and β-lactoglobulin interact with phenols resulting in a disordered secondary structure (Yang et al., 2021). Similarly, these interactions may lead to significant changes in protein function. For example, gallic acid expands the spatial structure of myofibrillar proteins, thereby altering the viscoelastic and structural properties of protein gels (Cao, True, Chen, & Xiong, 2016). In order to further increase the gel properties of proteins, Zhang et al. recently investigated the synergistic effect of transglutaminase (TG) and proanthocyanidin B2 (PCB2) on improving the springiness, hardness and structural compactness of oxidized MP gels (Zhang et al., 2022). The results demonstrated that the combination of TG and PCB2 could effectively improve gel formation. However, due to the spontaneous interaction between polyphenol antioxidants and proteins, a small amount of polyphenol addition has difficulties exerting its antioxidant

* Corresponding authors.
E-mail addresses: guijiechen@ahau.edu.cn (G. Chen), lix01@yctu.edu.cn (X. Li).

https://doi.org/10.1016/j.fochx.2024.101117
Received 24 October 2023; Received in revised form 12 December 2023; Accepted 1 January 2024
Available online 3 January 2024

effects, and a high concentration of polyphenol will consume too many sulfhydryls in myofibril, thus reducing the gelling property of MP. This suggests that polyphenol supplementation needs to be in a range of concentrations to have a positive effect. For example, chlorogenic acid at low and medium concentrations causes changes in the physicochemical properties of pork myofibrillar protein, promoting the protein's gelling ability, while at high concentrations it significantly inhibits the formation of MP gels (Cao & Xiong, 2015). For another example, Ultera et al. found in the metal-catalyzed tryptophan system that high-dose phenolic compounds had a strong oxidation-promoting effect (Utrera & Estévez, 2012). These results suggest that polyphenols may induce significant changes in the functional properties of gel-associated proteins, leading us to elucidate how and to what extent phenolic compounds affect their oxidation, water holding capacity and gel properties.

Black rice is very popular in China because it is rich in two flavonoid pigment anthocyanins, cyanidin-3-O-glucoside, along with peonidin-3-O-glucoside, which have superior antioxidant properties, biosafety and potential anti-aging effects (Li et al., 2019; Pedro, Granato, & Rosso, 2016). For example, Cassidy et al. found that intake of anthocyanins can effectively reduce the risk of diabetes and cardiovascular disease (Cassidy et al., 2013). Vemana et al. found that intestinal metabolites of black rice extract (BE) can significantly improve the antioxidant capacity of cells, and they believe that BE can be considered as a therapeutic agent against oxidative stress and diabetes (Gowd, Bao, & Chen, 2019). We have also previously demonstrated by transcriptomics that the black rice anthocyanin diet can modulate the normal expression of age-related genes and increase the lifespan of Drosophila melanogaster (Li et al., 2019). BE is cheap, easy to prepare on a large scale and has strong biological activity, however, the effects of BE on the oxidation and gel properties of meat have not been reported. Therefore, in order to investigate this gap, black rice extract was used in this investigation to evaluate its antioxidant properties and gel formation effects.

In this study, hydroxyl radicals were used to simulate the oxidation environment, and BE was used as an antioxidant. By measuring the effects of increasing concentrations of BE on the physicochemical properties of myofibrillar proteins, the free carbonyl groups, sulfhydryl groups, and secondary and tertiary structures of these modified proteins were investigated. At the same time, the water distribution and microstructure of myofibrillar gels were obtained to study the improvement of black rice extract on the three-dimensional network gel configuration. Finally, gel electrophoresis was used to evaluate the molecular weight of MP. In this study, the effects of BE on myofibrillar protein oxidation and gel formation were studied in order to provide a theoretical basis for the practical application of BE in meat production and processing.

2. Materials and methods

2.1. Materials and reagents

Fresh pork tenderloin (within 48 h after slaughter) was obtained from Yancheng Baolong Yonghui Supermarket. Guanidine hydrochloride, bomophenol blue, ethylenediamine tetraacetic acid (EDTA), 2, 4-dinitrophenylhydrazine (DNPH), dithiothreitol (DTT), and 2- nitrobenzoic acid (DTNB) were obtained from Aladdin (Shanghai, China). Black rice extract (Li et al., 2019) (main component: 83.89 % cyanidin-3-o-Glucoside, 3.12 % cyanidin-3,5-diglucoside, 5.45 % petunidin-3-O-glucoside) was purchased from Tianjin Jianfeng Natural Products Research and Development Co., Ltd.

2.2. Methods

2.2.1. MP extraction

Extraction procedure of MP from pork according to Cao and Xiong (2015). Briefly, 0.4 L of phosphate buffer (PBS, 0.02 mol/L) was added into 100 g lean minced meat. After homogenizing the turbid solution in an ice bath, the sample was centrifuged at 6797 g, 4 °C for 600 s, and the precipitate was washed 4 times with NaCl solution (0.1 mol/L) to obtain myofibrillar protein. A standard curve of bovine serum albumin was obtained, the MP concentration was determined by biuret method, and stored at 4 °C for later use.

2.2.2. MP oxidation

MP was oxidized according to the method of Cao et al. (2021). Different concentrations of BE (0, 10, 20 and 50 mg g^{-1}) were added to 40 mg mL^{-1} MP protein solution, and 1 mM H_2O_2, 100 μM ascorbic acid, and 10 μM $FeCl_3$ were added to oxidize MP at 4 °C for 24 h. MP oxidation samples containing different concentrations of BE were obtained, MP + 0 mg g^{-1} BE (NonOx), oxidant MP (Ox), oxidant MP + 10 mg g^{-1} BE (Ox + 10 BE), oxidant MP + 20 mg g^{-1} BE (Ox + 20 BE), oxidant MP + 50 mg g^{-1} BE (Ox + 50 BE). Another standard curve of bovine serum albumin was obtained and the final protein concentrations were determined by biuret method.

2.2.3. Determination of carbonyl content

The carbonyl content was measured according to the 2,4-Dinitrophenylhydrazine (DNPH) method of Xu, Yu, and Zeng (2021). 1 mL of MP solution (1 mg mL^{-1}) was mixed with 1 mL of DNPH (10 mmol/L), and incubated in the dark for 1 h (vortex oscillation every 300 s). At the end of the reaction, 1 mL of trichloroacetic acid (20 %) was combined with the mixture, and then centrifuged at 110 g and 4 °C for 300 s. The supernatant was discarded and sample cleaned with ethyl acetate - ethanol (1:1) for three times. 3 mL guanidine hydrochloride (6 M) was added and samples were shaken for 1200 s away from light to dissolve and precipitate. Samples were centrifuged at 10,620 g for 300 s to remove insoluble substances. Carbonyl content was calculated according to Lambert-Beer law with the sample absorbance of 370 nm.

2.2.4. Determination of sulfhydryl content

The content of sulfhydryl was determined according to the 5,5′-Dithiobis (2-nitrobenzoic acid) (DTNB – Ellmans reagent) procedure by Niu et al. (2020). Briefly, the final concentration of 500 μg mL^{-1} MP solution and 5 mM PBS containing 8000 mM urea, 600 mM NaCl, 10 mM (EDTA) was obtained. Thereafter, this solution was incubated at 40 °C for 0.5 h after adding DTNB (final concentration 1 mg mL^{-1}). The absorption value at 412 nm was obtained to calculate the sulfhydryl content.

2.2.5. Determination of solubility

MP's solubility was determined according to the method of Cheng, Zhu, and Liu (2020). Briefly, the supernatant of MP (1 mg mL^{-1}) was obtained from centrifugation, and the solubility was calculated by the changes of protein content.

2.2.6. FTIR

The freeze-dried sample (1 mg) was firstly ground into powder with potassium bromide (130 mg). Then, the powder is quickly transferred to a mold and pressed. The obtained transparent sample piece was scanned to obtain Fourier infrared spectra: wavenumber range: 400–4000 cm^{-1}; scan rate: 0.2 cm/s. The resolution of each spectrum was 4 cm^{-1} with 64 scans.

2.2.7. Fluorescence spectra

Samples (0.4 mg mL^{-1}) were prepared by dissolving NonOx, Ox, Ox + 10BE, Ox + 20BE, and Ox + 50BE in 0.6 M NaCl PBS. The fluorescence changes of tryptophan in various samples were measured by fluorescence spectrometer with the 295 nm of excitation wavelength and 300–400 nm of emission spectrum. Both excitation and emission slit widths were 10 nm.

2.2.8. Surface hydrophobicity

Surface hydrophobicity was determined by the method of a previous study (Zhang, Jing, Sun, Meng, & Yang, 2018). 1 mL MP solution (5 mg

mL^{-1}) and 0.2 mL bromophenol blue solution (BPB; 1 mg mL^{-1}) were mixed and shaken for 600 s. The combined solution was centrifuged at 8000 g for 900 s, and the supernatant was taken and diluted 10 times with 0.02 mol PBS. The absorption value was determined at 595 nm. 1 mL PBS was combined with 0.2 mL bromophenol blue solution as the control group.

2.2.9. Preparation of MP gel

Sample solutions (40 mg/mL) was placed on a Petri dish with a diameter of 2.5 cm. Petri dishes and water baths were incubated at 1 °C min^{-1} at 30–80 °C and incubated in 80 °C water bath for 20 min. Samples were removed, cooled immediately in ice water, and stored for later use.

2.2.10. Measurement of rheological properties of MP gels

The dynamic rheology was measured using methods by Khalesi, Sun, He, Lu, and Fang (2021). The MP solution (40 mg mL^{-1}) was placed on a heated plate (upper plate diameter 30 mm, lower plate diameter 50 mm, gap 1 mm). When the temperature of 1 °C min^{-1} increased from 30 °C to 90 °C, the force generated by the sample was recorded under the shock mode with a fixed frequency of 0.1 Hz and a stress force of 0.1.

2.2.11. The texture of the gel

The texture of the gel was determined according to Zhou et al. (2023). The prepared gel samples were placed at 25 °C for 0.5 h, and the gel strength was obtained by TA-XT Plus texture meter (Shimadzu). Texture parameters: Rate before test 2.0 mm s^{-1}; Trigger force 5.0 g; Test rate 1 mm s^{-1}; Return rate 2.0 mm s^{-1}.

2.2.12. Determination of water holding capacity (WHC) of gels

MP gel was set at 25 °C for 0.5 h, and 5 g of samples were centrifuged at 5000 rpm for 15 min. After removing moisture, weigh m_1 to calculate WHC according to the formula below.

$$WHC = (5 - m_1)/5$$

2.2.13. LF-NMR determination of gels

It is performed according to the method from Shen, Stephen Elmore, Zhao, and Sun (2020). The relaxation time (T2) of the gel mixture was measured by NM120 low-field NMR analyzer. Parameter setting: temperature 32.00 ± 0.01 °C; Frequency 22.6 MHz; Scan 32 times; Echo number 12,000; RG1 = 10 bd; P1 = 6 μs; DRG = 4; TW = 3000 ms; TE = 1.5 ms. MRI is measured by magnetic resonance imaging. Multiple spin echo (MSE) imaging sequences were used to analyze proton density imaging of MP gel. Parameters were set to image repetition time TR = 1000 ms, echo time TE = 20 ms, center frequency SF = 24 MHz. False-color images were obtained from proton density images and water distributions.

2.2.14. Microstructure imaging of a MP gel

The SEM of MP gel was determined according to Zhou, Zhao, Zhao, Sun, and Cui (2014). The gel sample block was fixed in 2.5 % glutaraldehyde for 24 h. The fixed sample was washed with 0.1 mol PBS for 20 min, then dehydrated sequentially in gradient ethanol (50, 60, 70, 80, 90, 95, 100 % ethanol/water) three times for 10 min each time. Imaging was performed by SEM (Hitachi Hi-tech Co., Ltd., SU1510, Japan).

2.2.15. SDS-PAGE

The electrophoresis of MP gel was done as performed by Cao and Xiong (2015). The gel sample was homogenized in 5 % SDS solution to prepare 5 mg/mL MP suspension with or without 5 % dithiothreitol (DTT, disulfide bond severing). The sample was then boiled for 5 min. The concentration of separation gel and loading gel was 12 % and 5 %, respectively. 3 h after electrophoresis, Coomassie bright blue staining, glacial acetic acid and methanol destaining were used before gel imaging.

2.3. Statistical analysis

All experiments were repeated three times and expressed as mean ± standard deviation (SD). SPSS statistical software (IBM SPSS Statistics 19) was used for data analysis. Univariate analysis of variance was used for statistical analysis, and the Duncan test was used ($P < 0.05$) to determine if the experimental difference was statistically significant.

3. Results and discussion

3.1. Effect of BE on physicochemical properties of MP

3.1.1. The content of carbonyl and sulfhydryl groups

In the presence of oxidants or free radicals, the amino acid side chains of proteins are easily modified by non-enzymatic irreversible oxidation. These oxidative modifications can result in loss of sulfhydryl groups and formation carbonyl groups, and it will further cause protein polymerization and depolymerization, change the secondary and tertiary structure of protein, and thus change the physical properties, such as surface hydrophobicity, etc. (Chen et al., 2016; Feng et al., 2015). As shown in Fig. 1a, compared to unoxidized MP, carbonyl content in oxidized MP increased by 33.8 % ($P < 0.05$). The addition of BE in MP can effectively reduce the formation of carbonyl groups and show a concentration-dependent effect. This may be attributed to the active hydroxyl groups of polyphenols, which can scavenge overproduced ROS or isolate the metal oxide to protect the original properties of amino acids. This is similar to the results of previous studies that polyphenols inhibit the formation of MP carbonyls, such as adding blackcurrant extract to raw pork pie (Jia, Wang, Shao, Liu, & Kong, 2017), and cooking pork pie with rapeseed and pine bark extract (Vuorela et al., 2005). In protein molecules, the high content of sulfhydryl groups plays an important role in the stability of MP structure. However, they are highly reactive and easily oxidized into disulfide bonds (—S—S—). The content of sulfhydryl groups in the unoxidized MP reached 9.1 μmol g^{-1} (Fig. 1b). However, the content of MP sulfhydryl groups after oxidation decreased by 9.9 %, indicating that oxidation caused significant loss of sulfhydryl groups, which was consistent with a previous study (Cao et al., 2016). Surprisingly, the addition of BE had no protective effect on MP's sulfhydryl groups (Fig. 1b). The possible reasons are as follows: (1) Covalent bonds may form between BE and proteins. Quinone intermediates are formed after oxidation of phenolic substances, which react easily with MP's sulfhydryl groups (nucleophilic groups) to form a complex; (2) The addition of BE led to the expansion of MP structure, which further turns more sulfhydryl groups into —S—S—.

3.1.2. Hydrophobic properties

Changes in MP structure may affect its hydrophilic and hydrophobic abilities. As such, bromophenol blue (BPB) reagent was used to investigate the effects of oxidation treatment and BE addition on the hydrophobic capacity of MP. Protein hydrophobic amino acid residues can bind BPB to form color substrates. Therefore, more BPB binding indicates more hydrophobic protein surface available. As shown in Fig. 1c, surface hydrophobicity of MP was enhanced after oxidation. In addition, the addition of BE further improves the surface hydrophobicity of MP (Fig. 1c). The increase of protein surface hydrophobicity may be attributed to the interaction between BE and MP, which changes protein spatial conformation. This effect is similar to the conclusions previously reported for the addition of phenolic compounds to MP (Dai et al., 2020). Hydrophobic interaction is the important factor in promoting the formation of gel (Zhang et al., 2022). Therefore, an appropriate increase of hydrophobicity can make more hydrophobic groups participate in the thermal gel formation process, which may be conducive to the improvement of gel properties. The increase of protein surface hydrophobicity and the formation of many disulfide bonds will further reduce MP solubility (Zhang et al., 2018). As shown in Fig. 1d, compared with MP without oxidation treatment, the solubility of oxidized MP was

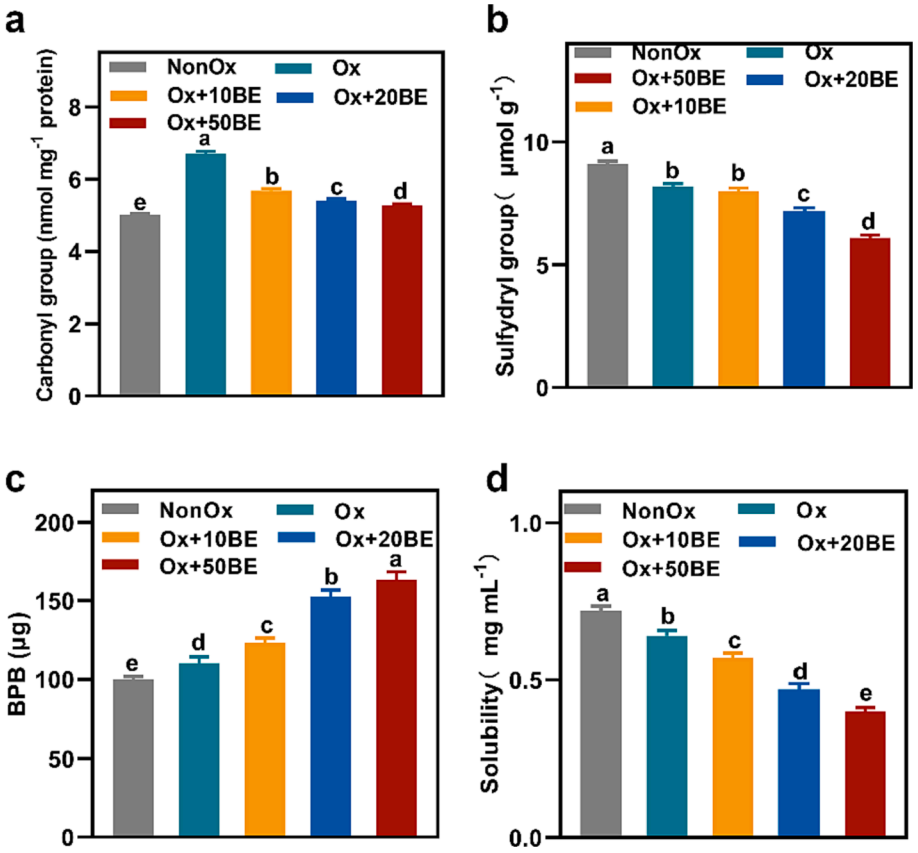

Fig. 1. Effect of BE on physicochemical properties of MP. a) The content of carbonyl group of MP treated with different concentration of BE; b) the content of sulfydryl group of MP treated with different concentration of BE; c) the combination of bromophenol blue (BPB) with MP treated with different concentration of BE; d) the solubility of MP treated with different concentration of BE. Data was expressed as mean ± SD (n = 3). Different lowercase letters indicate significant differences ($P < 0.05$). (For interpretation of the references to color in this figure legend, the reader is referred to the web version of this article.)

reduced by 11.1 % ($P < 0.05$). The addition of BE resulted in further reduction of MP solubility in a dose-dependent manner. A previous study also indicated that the addition of polyphenols (−)-Epigallocatechin gallate (EGCG) decreased the solubility of MP (Zhang, Yang, & Acevedo, 2020). This effect may be due to the reduction of protein solubility via the covalent cross-linking products of sulfhydryl and quinone. This indicates that increasing the amount of BE may lead to MP aggregation.

3.1.3. Effects of BE on the structure of MP

We further analyzed the changes of functional group in MP by FTIR. As shown in Fig. 2a, MP with different concentration of BE showed a similar FTIR spectrum, indicating that there was no significant change in the number of chemical bonds.The peaks at 3500–3200 cm^{-1} are attributed to the stretching vibration of C—H (Amide A). Compared with unoxidized MP samples, the peak width (Amide A) of oxidized MP samples was reduced, indicating that oxidized MP has lower C—H.These peaks at 1700–1600 cm^{-1} are usually attributed to the C═O stretching, peptidyl C—N stretching, additionally Cα-c-N bending and N—H in-

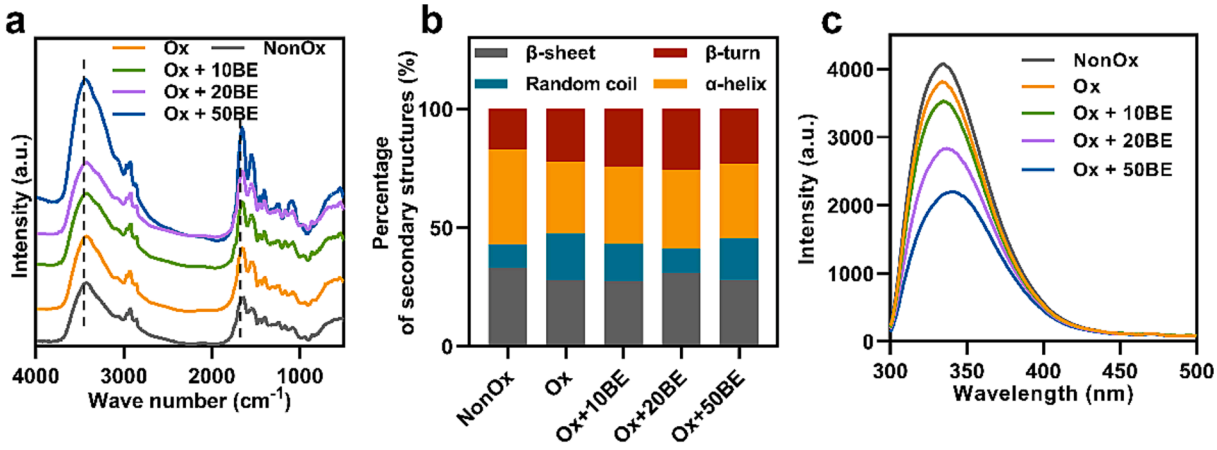

Fig. 2. Effect of BE on the structure of MP. a) FTIR spectra; b) the secondary structure information extracted from 1700 to 1600 cm^{-1}; c) the fluorescence spectra of intrinsic tryptophan.

plane bending patterns (Amide I) (Signorelli, Cannistraro, & Bizzarri, 2019), and they are always used to evaluate the secondary structure of proteins. There were slight changes in peak shape and position in Amide I. This suggests oxidation process and BE addition may change the secondary structure of MP (Fig. 2a). Detailed secondary structure information extracted from 1700 to 1600 cm^{-1} was shown in Fig. 2b. Compared with unoxidized MP, the α-helix content of oxidized MP decreased, while the β-turn and random curling contents increased. The addition of BE can stabilize the helical structure of the protein. For example, there was a 10 % increase in α-helix in the Ox + 20BE group compared to oxidized MP. This indicates that moderate BE causes an increase in the order of MP structure. However, compared with Ox + 20BE group, 50 mg g^{-1} of BE reduced the α-helical content and increased the disordered structure, thus reducing the order of MP.

The difference in MP's hydrophilic and hydrophobic properties suggest the change of amino acid microenvironment. The tryptophan fluorescence in protein is receptive to the change of microenvironment, so the tertiary structure of MP can be evaluated by monitoring tryptophan fluorescence intensity (Feng, Yin, Zhou, Ma, & Zhang, 2023). Fig. 3c shows that the fluorescence intensity of oxidized MP obviously decreased. This may be that oxidative stress accelerates the structural expansion of MP, and make the tryptophan exposed (hydrophobic environment). In addition, BE supplementation led to a further decrease in the fluorescence intensity of tryptophan. This effect is similar to Dai et al. using rosmarinic acid to reduce the fluorescence intensity of MP (Dai et al., 2020). It suggests that the phenolic compounds may be interacting with tryptophan residues, thus reducing their fluorescence properties. In addition, the binding of BE to tryptophan residues may also play a role in energy resonance transfer, resulting in a reduction of emission intensity by tryptophan.

3.2. Effect of BE on properties of MP gel

3.2.1. Dynamic rheology

Dynamic rheology can sensitively detect gel formation in a non-destructive manner. In this study, the storage modulus (G') of MP during heating was measured by dynamic rheology. Disulfide bond formation of MP gel mainly occurred at 50–60 °C (Liu, Zhao, Xie, & Xiong, 2011). G' of unoxidized MP samples showed a typical initial increase at 40 °C and reached an excessive peak at 48 °C (Fig. 3a). This phenomenon can be attributed to the deformation and aggregation of MP molecular heads, exposing hydrophobic residues as precursors of gel formation (Cao et al., 2016). In addition, this suggests proteins aggregation and the formation of elastic networks. With the further increase of temperature, G' of MP samples decreased first and then increased continuously. It may be attributed to the further cross-linking and aggregation of protein and form a permanent, irreversible and stronger network structure (Jia et al., 2017). Compared with unoxidized MP, the peak value of oxidized MP decreased significantly at 48 °C, indicating that the MP head-to-head interaction was inhibited and the gel performance was reduced (Fig. 3a). The addition of Ox + 10BE and Ox + 20BE significantly increased the G' of oxidized MP. This may be due to BE's polyphenol active groups promoting the expansion of MP molecules, making more functional groups undergo the aggregation and gelation process, enhancing the cross-linking between protein–protein and protein-BE molecules, and leading to the formation of an irreversible heat-induced gel structure (Dai et al., 2020) (Fig. 3a). These results indicated that BE not only promoted the formation of MP gel, but also improved the physical properties of the gel. On the contrary, Ox + 50BE reduces the G' of MP (Fig. 3a). This may be due to the reaction from an overabundance of quinone groups formed by oxidation with sulfhydryl groups of proteins to form quinone-sulfhydryl complexes, which significantly reduces the content of sulfhydryl groups in MP molecules, thus inhibiting the construction of the three-dimensional network

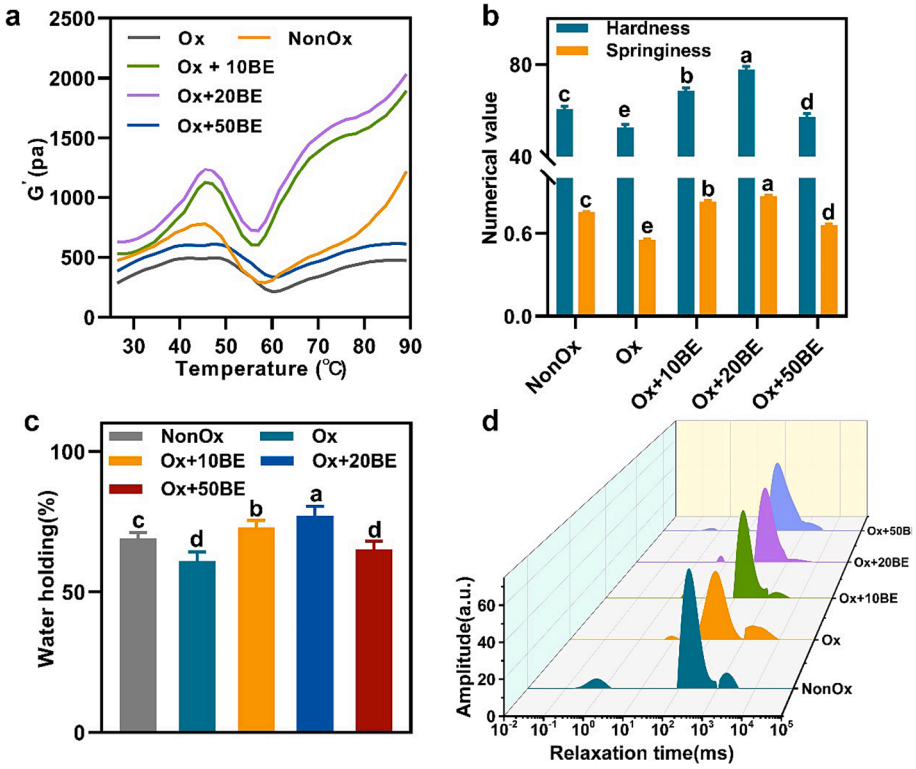

Fig. 3. Effect of BE on properties of MP gel. a) The storage modulus (G') of MP gel treated with different concentration of BE during heating; b) the hardness and springiness of MP gel treated with different concentration of BE (n = 3); c) the water holding capacity of MP gel treated with different concentration of BE (n = 3); d) LF-NMR results of MP gel treated with different concentration of BE. Different lowercase letters indicate significant differences ($P < 0.05$).

assembly of MP gel.

3.2.2. Hardness and springiness of MP gel

The effects of BE on the composition of oxidized MP gel are shown in Fig. 3b. Compared to the unoxidized MP gel, the hardness and springiness of oxidized MP gel decreased by 13 % and 26 %, respectively, indicating that the texture properties of oxidized MP gel decreased significantly. This effect can be attributed to the excessive cross-linking reaction caused by oxidation, leading to a large amount of protein aggregation. As a result, the ordered interaction between active functional groups is blocked. These lead to a reduced degree of binding between different proteins, proteins and water, inhibiting the formation of dense gel networks (Zhang et al., 2020). Low and medium doses of BE (Ox + 10BE and Ox + 20BE, respectively) can effectively increase the springiness and hardness of MP gel. On the one hand, the antioxidant capacity of BE reduces the formation of protein carbonyls and improves the performance of MP gel. On the other hand, BE promotes the development of MP structure, strengthens the hydrogen bonds and hydrophobic interactions in MP gel, and thus promotes the gel formation. However, a high dose of BE (Ox + 50BE) can hinder this gel formation, thus reducing its texture properties. This may be due to the formation of intramolecular —S—S— in MP, and the reduction of intermolecular disulfide bonds, thus inhibiting the formation of 3D network assembly and reducing the hardness and springiness of the resulting gel.

3.2.3. WHC of MP gel

The water holding capacity (WHC) is an important parameter in the study of gel properties (Zhou, Zhang, Lorenzo, & Zhang, 2021). Fig. 3c shows lower WHC in oxidized MP group compared to unoxidized MP, which is possibly due to the formation of disulfide bonds caused by oxidation, further preventing the assemble of 3D gel structure (Dai et al., 2020). Medium and low concentrations of BE significantly enhanced the WHC of oxidized MP. This effect occurs through BE changes to the gel structure of the protein through covalent and non-covalent interactions with the protein, thus increasing the WHC of MP. High dosage (Ox + 50BE), however, significantly decreased the WHC of MP gel ($P < 0.05$), which occurs because excessive BE significantly reduces the content of sulfhydryls in MP molecules, thus hindering the formation of three-dimensional gel network structure, and thus increasing the loss of bound water.

3.2.4. LF-NMR results

Subsequently, T_2 values which can reflect the allocation and displacement of water in the gel were measured by low field NMR (LF-NMR). MP gels appeared in 4 various water types at 0.1 ~ 1 ms (T_{2b}), 1 ~ 10 ms (T_{21}), 100 ~ 1000 ms (T_{22}) and 1000 ~ 1000 ms (T_{23}) (Cao et al., 2021). The peak gel relaxation time varies due to the microenvironment surrounding the water molecule. These four water types can be divided into three kind of water phases, namely, bound water, immobilized water and free water. T_{2b} and T_{21} peaks correspond to bound water. T_{22} and T_{23} readings correspond to immobilized water and free water, respectively. As shown in Table 1, compared with unoxidized MP gels, oxidized MP have an increased T_{22} (180–230 ms), decreased T_2 peak value area proportion (PT_{22}) (85–78 %), and increased PT_{23} (7 %–17 %). Protein oxidation can obstruct the formation of MP gel network arrangement and increases the loss of H_2O. This is similar with the texture properties of MP gel and the findings of the WHC study. Shen et al. also found an increasing loss of water molecules in porcine muscle fibrin gel under oxidation (Shen et al., 2020). However, the area between 100 ~ 1000 ms and 1000 ~ 10,000 ms increased indicated that Ox + 10BE and Ox + 20BE improved the water distribution of MP gels (Fig. 3d). On the one hand, the addition of BE promotes the formation of the oxidation network structure of MP gel. On the other hand, BE potentially raises the exposure of amino acid side chain groups in protein and enhance the interactions between MP and phenolic substances (Li et al., 2021). However, the area between 100 ~ 1000 ms and 1000 ~ 10,000 ms decreased indicated the Ox + 50BE group increased the conversion of bound water to free water in MP gel. This could be that 50 mg g^{-1} BE prevented the formation of the gel mesh structure, resulting in an increase in free water.

3.2.5. MRI results

MRI images visually show the water transfer of MP gel. Fig. 4 shows different states of water identified through various false color photos. Green areas are free water, while red areas represent bound or immobilized water (Zhou et al., 2021). The oxidized gel is green, indicating that the content of free water increases. After adding medium and low dose of BE, these gels showed a strong bright red signal, indicating the immobilized or bound water content increased. This may be because Ox + 10BE and Ox + 20BE promoted the formation of MP gel networks, and a large quantity of water is confined in the gel network, enhancing the interactions between water and proteins. However, the MP color of Ox + 50BE treatment was green, indicating increased free water. This is consistent with these results obtained by WHC, and LF-NMR.

3.2.6. SEM results

The gel morphology of NonOx, Ox + 10BE, Ox + 20BE and Ox + 50BE were observed by SEM. The oxidized MP gel failed to form an ordered network (Fig. 5). It may be due to the transition of sulfhydryl groups into —S—S— by oxidation, which decreased the interactions between proteins. Ox + 10BE and Ox + 20BE promoted the conformation of MP gel dense reticular structure. This is because appropriate BE increases the unfolding of MP structure, promotes the interaction between proteins, and forms an ordered gel structure during heating. However, Ox + 50BE decreased the density of reticular structure. The dense network is associated with a lower relaxation time (T_2), due to the smaller pore size of the network structure, which limits the movement of the water molecules and thus allows faster spin energy exchange with the peripheral water molecules. It is similar to the conclusion of Wang et al. (Wang et al., 2021) that oat fiber makes duck myofibrillar protein gel have a homogeneous and ordered flaky network structure. In addition, the dense reticular structure improved the structural properties of the gel, which is consistent with the results of dense reticular structure increasing WHC.

3.2.6. SDS-PAGE results

The crosslinking characteristics of MP treated with BE were evaluated by electrophoresis. As shown in Fig. 6a, it can be observed that

Table 1
Relaxation time and peak area percentage of MP with and without BE treatment.

	T_2 (park value)				PT_2 (T_2 park value area proportion) %			
Groups	T_{2b}/ms	T_{21}/ms	T_{22}/ms	T_{23}/ms	PT_{2b}/%	PT_{21}/%	PT_{22}/%	PT_{23}/%
NonOx	0.235 ± 0.013^{a}	5.434 ± 0.022^{d}	180.64 ± 2.151^{b}	1162.322 ± 61.564^{c}	0.352 ± 0.023^{b}	7.102 ± 0.122^{a}	85.04 ± 0.453^{d}	7.858 ± 0.892^{c}
Ox	0.144 ± 0.012^{a}	3.423 ± 0.033^{e}	230.14 ± 5.242^{a}	2612.675 ± 75.251^{a}	0.247 ± 0.032^{d}	4.201 ± 0.132^{b}	78.595 ± 0.232^{e}	17.204 ± 0.751^{a}
Ox + 10BE	0.514 ± 0.022^{a}	8.423 ± 0.052^{c}	173.419 ± 4.232^{c}	1742.633 ± 60.443^{d}	0.389 ± 0.042^{a}	$2.689 \pm 0.145c$	90.611 ± 0.524^{b}	6.695 ± 0.886^{d}
Ox + 20BE	1.111 ± 0.0434^{a}	27.256 ± 0.315^{a}	143.437 ± 2.156^{d}	1611.652 ± 65.524^{e}	0.404 ± 0.022^{a}	2.789 ± 0.115^{c}	91.239 ± 0.474^{a}	5.968 ± 0.446^{e}
Ox + 50BE	1.317 ± 0.037^{a}	10.326 ± 0.115^{b}	183.491 ± 2.246^{b}	1889.652 ± 51.435^{b}	0.291 ± 0.032^{c}	1.995 ± 0.145^{d}	89.852 ± 0.354^{c}	8.149 ± 0.753^{b}

Data was expressed as mean ± SD (n = 3). Different lowercase letters indicate significant differences ($P < 0.05$).

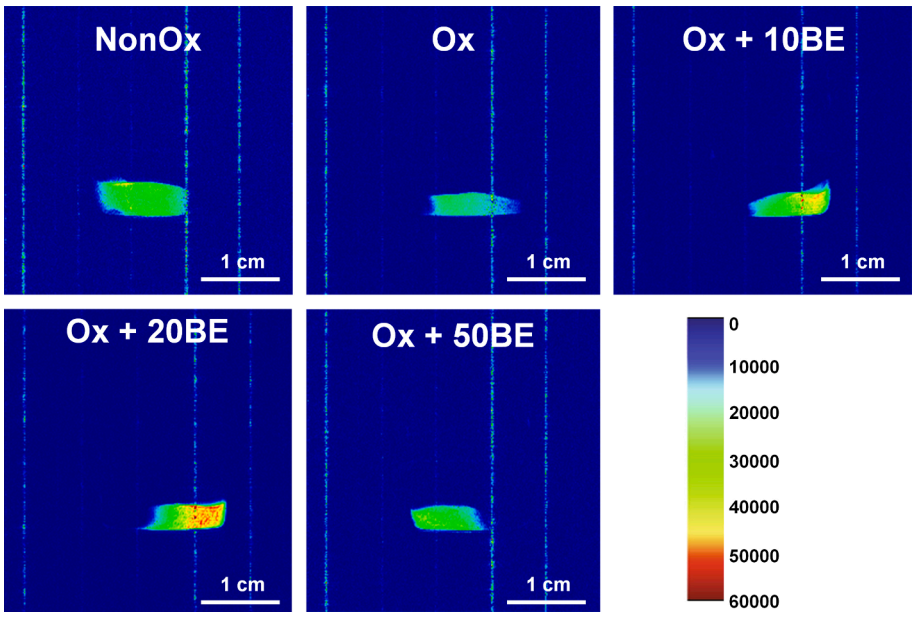

Fig. 4. MRI results of MP gel treated with different concentration of BE. Green areas (low signal strength) are free water, while bright or red areas (high signal strength) are bound or immobile water. (For interpretation of the references to color in this figure legend, the reader is referred to the web version of this article.)

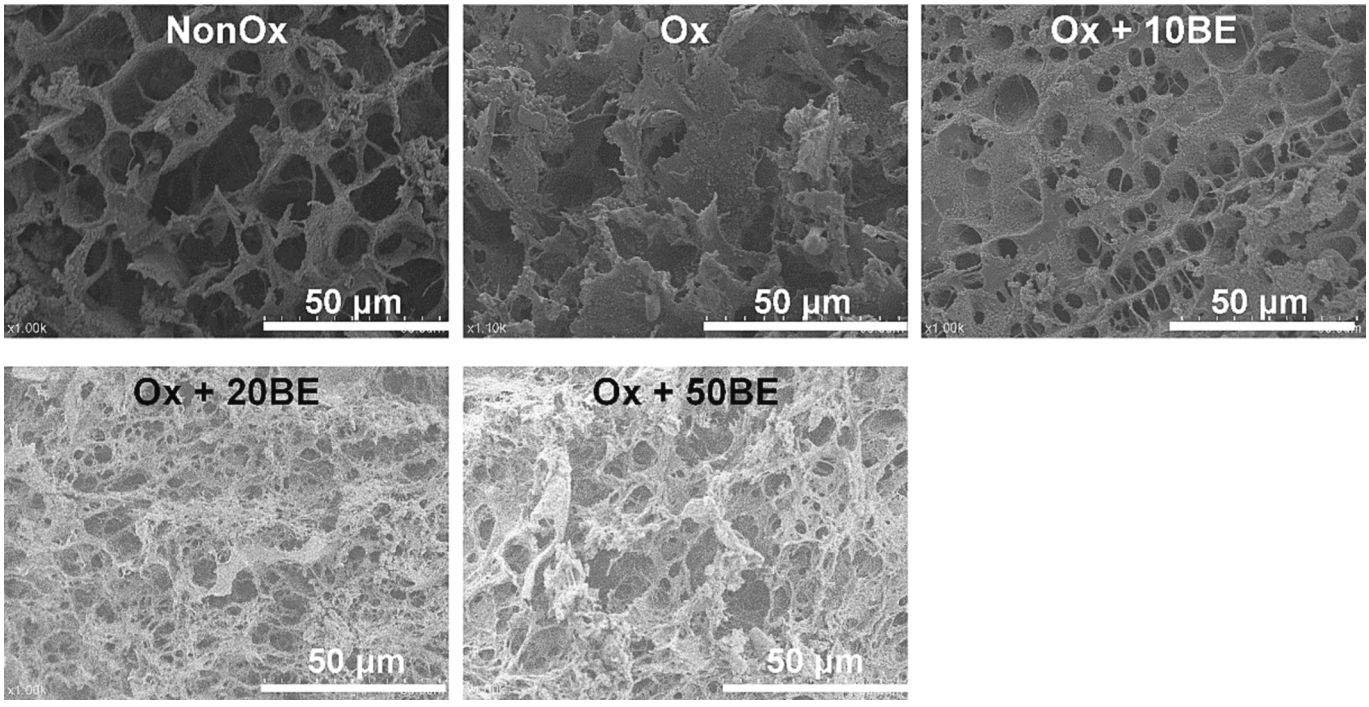

Fig. 5. The gel morphology of MP gel treated with different concentration of BE.

there is only MP heavy chain (MHC) in the lane. This is that the formation of MP gel under heating caused the cross-linking of protein light chain molecules. In the gel sample supplemented with DTT in Fig. 6b, light chains of myofibrils with ~30 KDa appeared (Yin, Xing, & Zhang, 2023), which is because DTT breaks the —S—S— in MP gel. In addition, protein aggregation occurred at the top of the concentrated gel in Fig. 6a, while aggregation decreased in Fig. 6b. This is because MP forms disulfide and non-disulfide covalent bonds during heating. When DTT was added, the aggregation at the top of the loading gel was reduced, revealing that the disulfide bonds disappeared. In addition, the aggregation at the top of the loading gel in Fig. 6b may be quinone-sulfhydryl complexes.

4. Conclusion

The effects of various concentrations of BE on the physicochemical properties and gelling ability of oxidized MP were studied. The results showed that: (a) BE treatment significantly reduced the carbonyl content in oxidized MP group, which improved protein crosslinking, surface hydrophobicity, WHC and texture properties of gel. (b) Low and medium dose (Ox + 10BE, Ox + 20BE) significantly enhanced the G' of MP, and improved the density of oxidized MP gel network. (c) The results of LF-

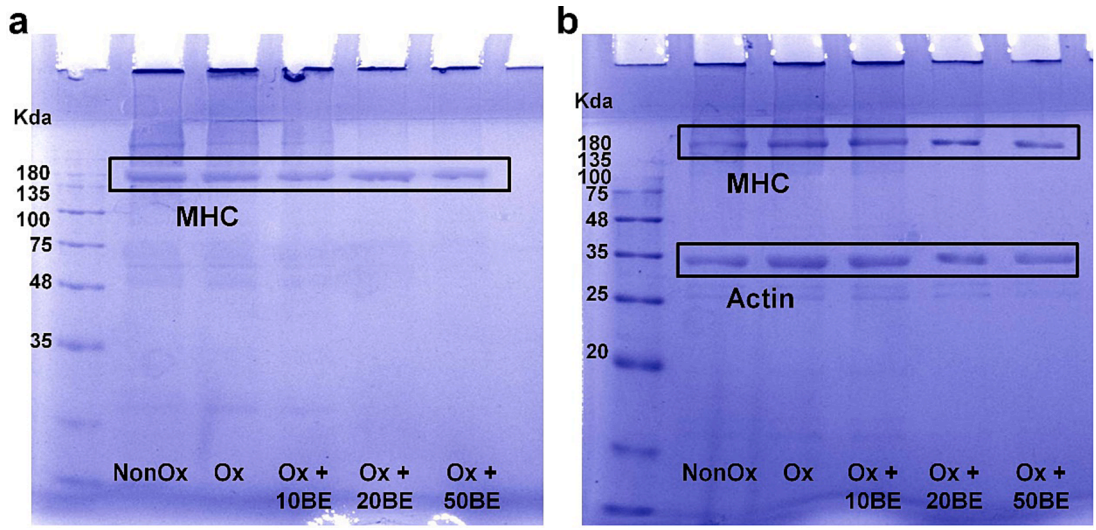

Fig. 6. SDS-PAGE results of MP gel treated with different concentration of BE. a) The MP treated without DTT; b) the MP treated with DTT.

NMR and MRI showed that Ox + 20BE could increase the binding ability between gel and water. In conclusion, an appropriate dosage of BE (20 mg g^{-1}) can significantly improve the capabilities of oxidized MP gel, providing a conceptual basis for a new antioxidant of meat products. Due to the low cost and easy availability of this antioxidant, it will have great applications in the processing and storage of meat products in the future.

CRediT authorship contribution statement

Huali Wang: Writing – original draft, Data curation, Conceptualization. **Matthew Kay:** Writing – review & editing. **Daojiu Zhang:** Software, Methodology. **Guijie Chen:** Software, Conceptualization. **Xiang Li:** Software, Project administration, Data curation, Conceptualization.

Declaration of competing interest

The authors declare that they have no known competing financial interests or personal relationships that could have appeared to influence the work reported in this paper.

Data availability

Data will be made available on request.

Acknowledgments

This study was supported by the National Natural Science Foundation Youth Fund (32001818), and the Open project of Jiangsu Key Laboratory for Bioresources of Saline Soils (JKLBS2020014).

References

Cao, Y., Li, B., Fan, X., Wang, J., Zhu, Z., Huang, J., & Xiong, Y. L. (2021). Synergistic recovery and enhancement of gelling properties of oxidatively damaged myofibrillar protein by -lysine and transglutaminase. *Food Chemistry, 358*, Article 129860.

Cao, Y., True, A. D., Chen, J., & Xiong, Y. L. (2016). Dual role (anti- and pro-oxidant) of gallic acid in mediating myofibrillar protein gelation and gel in vitro digestion. *Journal of Agricultural and Food Chemistry, 64*(15), 3054–3061.

Cao, Y., & Xiong, Y. L. (2015). Chlorogenic acid-mediated gel formation of oxidatively stressed myofibrillar protein. *Food Chemistry, 180*, 235–243.

Cassidy, A., Mukamal, K. J., Liu, L., Franz, M., Eliassen, A. H., & Rimm, E. B. (2013). High anthocyanin intake is associated with a reduced risk of myocardial infarction in young and middle-aged women. *Circulation, 127*(2), 188–196.

Chen, L., Li, C., Ullah, N., Guo, Y., Sun, X., Wang, X., Xu, X., Hackman, R. M., Zhou, G., & Feng, X. (2016). Different physicochemical, structural and digestibility characteristics of myofibrillar protein from PSE and normal pork before and after oxidation. *Meat Science, 121*, 228–237.

Cheng, J., Liu, D., Zhao, J., Li, X., Yan, Y., Wu, Z., Wang, H., & Wang, C. (2019). Lutein attenuates oxidative stress and inhibits lipid accumulation in free fatty acids-induced HepG2 cells by activating the AMPK pathway. *Journal of Functional Foods, 60*, Article 103445.

Cheng, J., Xu, L., Xiang, R., Liu, X., & Zhu, M. (2020). Effects of mulberry polyphenols on oxidation stability of sarcoplasmic and myofibrillar proteins in dried minced pork slices during processing and storage. *Meat Science, 160*, Article 107973.

Cheng, J., Zhu, M., & Liu, X. (2020). Insight into the conformational and functional properties of myofibrillar protein modified by mulberry polyphenols. *Food Chemistry, 308*, Article 125592.

Classics Lowry, O., Rosebrough, N., Farr, A., & Randall, R. (1951). Protein measurement with the Folin phenol reagent. *Journal of Biological Chemistry, 193*, 265–275.

Dai, H., Chen, X., Peng, L., Ma, L., Sun, Y., Li, L., Wang, Q., & Zhang, Y. (2020). The mechanism of improved myosin gel properties by low dose rosmarinic acid addition during gel formation. *Food Hydrocolloids, 106*, Article 105869.

Davies, M. J. (2016). Protein oxidation and peroxidation. *Biochemical Journal, 473*(7), 805–825.

Feng, F., Yin, Y., Zhou, L., Ma, C., & Zhang, W. (2023). Effect of nitric oxide and its induced protein S-nitrosylation on the structures and in vitro digestion properties of beef myofibrillar protein. *Journal of Agricultural and Food Chemistry, 71*(5), 2532–2540.

Feng, X., Li, C., Ullah, N., Hackman, R. M., Chen, L., & Zhou, G. (2015). Potential biomarker of myofibrillar protein oxidation in raw and cooked ham: 3-nitrotyrosine formed by nitrosation. *Journal of Agricultural and Food Chemistry, 63*, 10957–10964.

Fuentes-Lemus, E., & López-Alarcón, C. (2020). Photo-induced protein oxidation: Mechanisms, consequences and medical applications. *Essays in Biochemistry, 64*(1), 33–44.

Gowd, V., Bao, T., & Chen, W. (2019). Antioxidant potential and phenolic profile of blackberry anthocyanin extract followed by human gut microbiota fermentation. *Food Research International, 120*, 523–533.

Guo, A., & Xiong, Y. L. (2021). Myoprotein–phytophenol interaction: Implications for muscle food structure-forming properties. *Comprehensive Reviews in Food Science and Food Safety, 20*(3), 2801–2824.

Huang, X., Sun, L., Liu, L., Wang, G., Luo, P., Tang, D., & Huang, Q. (2022). Study on the mechanism of mulberry polyphenols inhibiting oxidation of beef myofibrillar protein. *Food Chemistry, 372*, Article 131241.

Jia, N., Wang, L., Shao, J., Liu, D., & Kong, B. (2017). Changes in the structural and gel properties of pork myofibrillar protein induced by catechin modification. *Meat Science, 127*, 45–50.

Khalesi, H., Sun, C., He, J., Lu, W., & Fang, Y. (2021). The role of amyloid fibrils in the modification of whey protein isolate gels with the form of stranded and particulate microstructures. *Food Research International, 140*, Article 109856.

Li, J., Munir, S., Yu, X., Yin, T., You, J., Liu, R., Xiong, S., & Hu, Y. (2021). Double-crosslinked effect of TGase and EGCG on myofibrillar proteins gel based on physicochemical properties and molecular docking. *Food Chemistry, 345*, Article 128655.

Li, X., Zhang, Z., Zhang, X., Cheng, J., Liu, D., Yan, Y., & Wang, H. (2019). Transcriptomic analysis of the life-extending effect exerted by black rice anthocyanin extract in D. melanogaster through regulation of aging pathways. *Experimental Gerontology, 119*, 33–39.

Li, X., Zhang, Z., Zhang, X., Yang, S., Liu, D., Diao, C., Wang, H., & Zheng, F. (2019). Cyanidin inhibits EMT induced by oxaliplatin via targeting the PDK1-PI3K/Akt signaling pathway. *Food & Function, 10*(2), 592–601.

Liu, R., Zhao, S., Xie, B., & Xiong, S. (2011). Contribution of protein conformation and intermolecular bonds to fish and pork gelation properties. *Food Hydrocolloids, 25*(5), 898–906.

Niu, F., Jiao, Y., Zhang, R., Fan, J., Ritzoulis, C., Pan, W., & Li, A. (2020). Properties of nano protein particle in solutions of myofibrillar protein extracted from giant squid (Dosidicusgigas). *Food Chemistry, 330*, Article 127254.

Pedro, A. C., Granato, D., & Rosso, N. D. (2016). Extraction of anthocyanins and polyphenols from black rice (Oryza sativa L.) by modeling and assessing their reversibility and stability. *Food Chemistry, 191*, 12–20.

Rosenfeld, M. A., Vasilyeva, A. D., Yurina, L. V., & Bychkova, A. V. (2018). Oxidation of proteins: Is it a programmed process? *Free Radical Research, 52*(1), 14–38.

Shen, H., Stephen Elmore, J., Zhao, M., & Sun, W. (2020). Effect of oxidation on the gel properties of porcine myofibrillar proteins and their binding abilities with selected flavour compounds. *Food Chemistry, 329*, Article 127032.

Signorelli, S., Cannistraro, S., & Bizzarri, A. R. (2019). Raman evidence of p53-DBD disorder decrease upon interaction with the anticancer protein azurin. *International Journal of Molecular Sciences, 20*(12), 3078.

Utrera, M., & Estévez, M. (2012). Analysis of tryptophan oxidation by fluorescence spectroscopy: Effect of metal-catalyzed oxidation and selected phenolic compounds. *Food Chemistry, 135*(1), 88–93.

Vuorela, S., Salminen, H., Mäkelä, M., Kivikari, R., Karonen, M., & Heinonen, M. (2005). Effect of plant phenolics on protein and lipid oxidation in cooked pork meat patties. *Journal of Agricultural and Food Chemistry, 53*(22), 8492–8497.

Wang, H., Yan, Y., Feng, X., Wu, Z., Guo, Y., Li, H., & Zhu, Q. (2020). Improved physicochemical stability of emulsions enriched in lutein by a combination of chlorogenic acid–whey protein isolate–dextran and vitamin E. *Journal of Food Science, 85*(10), 3323–3332.

Wang, Z., Sun, Y., Dang, Y., Cao, J., Pan, D., Guo, Y., & He, J. (2021). Water-insoluble dietary fibers from oats enhance gel properties of duck myofibrillar proteins. *Food Chemistry, 344*, Article 128690.

Xu, Q., Yu, Z., & Zeng, W. (2021). Structural and functional modifications of myofibrillar protein by natural phenolic compounds and their application in pork meatball. *Food Research International, 148*, Article 110593.

Yan, Y., Zhu, Q., Diao, C., Wang, J., Wu, Z., & Wang, H. (2020). Enhanced physicochemical stability of lutein-enriched emulsions by polyphenol-protein-polysaccharide conjugates and fat-soluble antioxidant. *Food Hydrocolloids, 101*, Article 105447.

Yang, W., Qu, X., Deng, C., Dai, L., Zhou, H., Xu, G., Li, B., Yulia, N., & Liu, C. (2021). Heat sensitive protein-heat stable protein interaction: Synergistic enhancement in the thermal co-aggregation and gelation of lactoferrin and α-lactalbumin. *Food Research International, 142*, Article 110179.

Yin, Y., Xing, L., & Zhang, W. (2023). Moderate protein oxidation improves bovine myofibril digestibility by releasing peptides in the S2 region of myosin: A peptidomics perspective. *Journal of Agricultural and Food Chemistry, 71*(5), 2514–2522.

Zhang, D., Yang, X., Wang, Y., Wang, B., Wang, S., Chang, J., Liu, S., & Wang, H. (2022). Proanthocyanidin B2 and transglutaminase synergistically improves gel properties of oxidized myofibrillar proteins. *Food Chemistry, 391*, Article 133262.

Zhang, L., Jing, E., Sun, Y., Meng, X., & Yang, Y. (2018). Optimization of GABA accumulation in brown rice under NaCl stress and Calcium regulation. *Food Research and Development, 39*, 7–14.

Zhang, M., Yang, Y., & Acevedo, N. C. (2020). Effects of pre-heating soybean protein isolate and transglutaminase treatments on the properties of egg-soybean protein isolate composite gels. *Food Chemistry, 318*, Article 126421.

Zhou, F., Zhao, M., Zhao, H., Sun, W., & Cui, C. (2014). Effects of oxidative modification on gel properties of isolated porcine myofibrillar protein by peroxyl radicals. *Meat Science, 96*(4), 1432–1439.

Zhou, L., Jiang, J., Feng, F., Wang, J., Cai, J., Xing, L., Zhou, G., & Zhang, W. (2023). Effects of carboxymethyl cellulose on the emulsifying, gel and digestive properties of myofibrillar protein-soybean oil emulsion. *Carbohydrate Polymers, 309*, Article 120679.

Zhou, L., Zhang, J., Lorenzo, J. M., & Zhang, W. (2021). Effects of ultrasound emulsification on the properties of pork myofibrillar protein-fat mixed gel. *Food Chemistry, 345*, Article 128751.